



# Design and analysis of a tracking / backtracking strategy for PV plants with horizontal trackers after their conversion to agrivoltaic plants



F.J. Casares de la Torre <sup>a</sup>, Marta Varo <sup>b,\*,1</sup>, R. López-Luque <sup>b</sup>, J. Ramírez-Faz <sup>a</sup>,  
L.M. Fernández-Ahumada <sup>a</sup>

<sup>a</sup> Department of Electrical Engineering and Automatics, University of Cordoba, Campus of Rabanales, 14071, Cordoba, Spain

<sup>b</sup> Department of Applied Physics, Radiology and Physical Medicine, University of Cordoba, Campus of Rabanales, 14071, Cordoba, Spain

## ARTICLE INFO

### Article history:

Received 26 October 2021  
Received in revised form  
20 December 2021  
Accepted 20 January 2022  
Available online 25 January 2022

### Keywords:

Agrivoltaics  
Photovoltaics  
N–S horizontal single-axis trackers  
Tracking / backtracking  
Dual land use  
Sustainability

## ABSTRACT

World population growth is leading to an increased demand for energy and food. This is creating a conflict over land use as terrain for large renewable energy facilities is not available for agricultural. As a solution, agrivoltaics combines the use of the land for agricultural and photovoltaic exploitation. In this work, the conversion of photovoltaic installations with N–S horizontal trackers into agrivoltaic installations by cultivating tree crops in hedgerows between the rows of collectors is analysed. Specifically, the shading of the crop on the photovoltaic panels is studied. It has been proved that there is an area between the collectors in which the crop would not shade the photovoltaic panels. Likewise, a new tracking/backtracking strategy is proposed to avoid shading in cases where the crop exceeds this region of no influence. Finally, it has been found that the Land Equivalent Ratio for an agrivoltaic plant in Córdoba (Spain) with N–S horizontal trackers and olive groves in hedges up to 3.0 m high and 1.5 m wide can increase between 28.9% and 47.2%. Thus, these PV installations are potentially adaptable to agrivoltaic installations making renewable energy facilities compatible with a more efficient and sustainable agricultural model.

© 2022 The Authors. Published by Elsevier Ltd. This is an open access article under the CC BY license (<http://creativecommons.org/licenses/by/4.0/>).

## 1. Introduction

The world population has been growing in recent years and it is expected that the current 7.7 billion people will reach 8.5 billion in 2030 or 9.7 billion in 2050 [1]. As a consequence, the needs of society worldwide also increase [2]. Thus, for example, at the energy level, the demand for electricity has been growing very rapidly in recent years and it is expected that this growth will not slow down in 2021 and 2022 (increases of almost 1200 TWh and 1000 TWh respectively) after the decrease caused by COVID 19 in 2020 (almost 500 TWh less than the previous year) [3]. This fact, together with the negative effects that conventional energies based on fossil fuels present for the environment, have encouraged the institutions to promote change towards a sustainable energy model where renewable energies are gaining prominence.

In this context, photovoltaic energy plays a very important role since it has important advantages such as its availability anywhere,

its easy installation, its low cost of maintenance and acquisition, its increased efficiency and its durability. Furthermore, these characteristics lead to a decrease in the LCOE (Levelized Cost of Energy) [4,5]. Hence the installed PV power in the world is increasing considerably. Thus, the new installations reached 139 GW in 2020 [6] and 117 GW are expected in 2021 and 119 GW in 2022 [7]. However, PV energy is not exempt from criticism since, traditionally, the large tracts of land that are dedicated to PV plants connected to the grid are no longer available for agri-food production. This fact affects negatively the possibilities of meeting the demand for food that also increases as a consequence of population growth [8], especially in areas with scarce land availability and high population density [9].

As a solution to this dilemma, agrivoltaics proposes to combine PV and agricultural production on the same land. For that purpose, PV panels are mounted at sufficient heights to allow agricultural cultivation under them. This concept was first proposed by Goetzberger and Zastrow in 1982 [10]. However, it was not put into practice in pilot agrivoltaic plants until three decades later [9]. Since then, although there are not many commercial or research facilities [9], plenty of studies have analysed the behaviour of

\* Corresponding author.  
E-mail address: [fa2vamam@uco.es](mailto:fa2vamam@uco.es) (M. Varo).

<sup>1</sup> Scopus Author ID: 56078356300

Nomenclature			
$a$	PV panel width	$\vec{s}$	solar vector
$a_c$	hedgerow crop width	$s_x, s_y, s_z$	components of solar vector
$a_p, b_p, F_1, F_2$	Pérez model parameters	$t$	solar hour
$d$	distance between two contiguous rows of PV panels	<i>Greek Letters</i>	
$d_j$	Julian day	$\beta$	inclination angle of the collector
$D$	distance from the upper vertex of the crop Q to the axis of the rear solar collector on which its shadow would be projected	$\beta_c$	corrected inclination of the collector to avoid the shadows of the crops
$h$	PV collector height	$\beta_{LG}$	maximum inclination angle of the collector for which the astronomical tracking does not imply intershading
$h_c$	hedgerow crop height	$\beta_{LT}$	technological limit inclination angle of the collector
$H_i$	daily incident radiation on the collector for the day $i$	$\Gamma$	daily angle
$H_y^{est}$	estimation of the annual incident radiation on the solar collectors	$\delta$	solar declination
$I$	incident irradiance on the collectors	$\eta_{AG-AGPG}$	agricultural efficiency in the agrivoltaic installation
$I_B$	direct solar irradiance on horizontal plane	$\eta_{PV-AGPG}$	photovoltaic efficiency in the agrivoltaic installation
$I_D$	diffuse solar irradiance	$\eta_{AG}$	yields of the land when it is exclusively dedicated to agricultural production
$I_{OH}$	horizontal extraterrestrial irradiance	$\eta_{PV}$	yields of the land when it is exclusively dedicated to photovoltaic production
$\vec{i}, \vec{j}, \vec{k}$	unit vectors associated to $O_{xyz}$ system	$\theta$	angle of incidence of sunbeams on the inclined plane
$LCOE$	Levelized Cost of Energy	$\theta_z$	solar zenith angle
$LER$	Land Equivalent Ratio	$\rho$	albedo
$M$	midpoint between the axis of the solar collectors	$\gamma$	apparent solar elevation
$\vec{n}$	normal vector to the solar collector	$\gamma_1$	delimiting apparent solar elevation angle when the whole collector is shaded by the crop
$Nd_j$	number of Julian days in the month $j$	$\gamma_2$	delimiting apparent solar elevation angle when the collector is partially shaded
$O_x, O_y, O_z$	axis of the horizontal reference system	$\gamma_3$	delimiting apparent solar elevation angle when the collector is not shaded
$P, T$	end points of PV panels in adjacent rows	$\gamma_{LG}$	limit apparent solar elevation
$Q$	Crop upper vertex nearer to the solar collector on which its shadow would be projected	$\psi$	latitude of the place
$R$	region between the rows of PV collectors in which crops that are included do not shade the solar collectors	$\Omega$	Earth's rotation speed
$r$	ratio of solar irradiance losses on an agrivoltaic plant with the proposed monitoring strategy compared to the capture of the plant without cropping		

agrivoltaic facilities, both from an agricultural and energy point of view [2,11–20].

With regard to crops, PV panels partially shade the crop and reduce incident irradiance levels on it, affecting crop production [2,9,14,17,18,21]. Simultaneously, the shading and the reduction of irradiance cause the temperature on the crop and on the land to decrease, thus protecting the crop from excessive heat [19]. In addition, partial shading can be beneficial for certain crops and could reduce water consumption by evapotranspiration and positively affect the water balance of the soil [2,13]. The benefits of partial shading on crop yield are also enhanced in time of drought. That is the reason why some authors affirm that agrivoltaics can strengthen the agricultural sector in the face of climate change [2,9]. In this regard, it is necessary to continue characterising the behaviour of different crops under agrivoltaic conditions to identify those that have better performance in these types of facilities.

Furthermore, it is important to note that the conditions of partial shading and incident irradiance on the crop can be varied depending on the design of the PV plant: height, orientation and density of panels or separation between rows of collectors [2,9,17]. Therefore, and given that these design variables also affect energy production, it is convenient to analyse in detail that configuration which optimises the combined agricultural and energy production of the agrivoltaic plant.

In this regard, various studies have shown that individually agricultural production decreases due to the reduction in the levels of solar irradiance incident on crops. Similarly, electricity power production also decreases due to having a lower density of PV panels that allow a good shade balance and irradiance on the crop. However, despite these individual production decreases, agrivoltaics increases the global economic performance of the land by combining agricultural and energy production [12,14,20,22]. To quantify this gain, the Land Equivalent Ratio (LER) [23] is used, comparing the yield of the land with agrivoltaic use (combined agricultural and energy production) with that of the use of the land for PV and agricultural production independently [14]. Different studies have estimated the LER for different agrivoltaic plants, finding that this variable is always greater than 1 [2,14], increasing in cases with solar monitoring and by increasing the density of panels [2]. In this line, Agostini et al. [11] have verified that the economic and environmental costs of agrivoltaic systems are comparable to those of other photovoltaic systems. However, the former present significant advantages over the latter since they favour the stabilisation of crop production with a lesser impact on land occupation. Likewise, Cuppari et al. [24] have developed a model to analyse whether agrivoltaics can reduce the financial risk related to weather conditions for farmers. Specifically, they verify, for the different cases studied, that annual net income always

increases in the case of agrivoltaics with respect to the exclusive agricultural use of the land, with an increase reaching up to 5000%. Additionally, agrivoltaic diversifies income streams, reducing risk and improving financial stability during volatile market and weather conditions. Therefore, agrivoltaic systems must be considered essential in a future energy system compatible with climate change and the energy and food needs of the growing world population.

Although the first research into agrivoltaics was limited to PV installations with fixed panels [18], recently other designs with solar trackers (mainly single-axis ones) have been analysed [2,9,12]. In that line of work, it has been proved that, not only is the energy production of the plant improved [12] but also the agricultural production of the cultivation [12,13,17,19]. Specifically, the use of mobile PV panels can be used to improve the distribution of rain in the crops under the panels [25] as well as to increase the solar incidence in the extreme hours of the day and reduce high temperatures at noon [12].

In this context, this work analyses the possibility of combining photovoltaic installations with modern modes of production in tree agriculture (olive, almond, peach, cherry, apple, pear) in hedges. This model of agricultural production has important advantages, such as the reduction of costs and labour thanks to the mechanisation of work, as well as the increase in production and the quality of the harvest. These improvements give rise to a higher profitability of the land [26]. Thus, this agricultural model would make it possible to reconcile tree cultivation with agrivoltaics, until now limited to low-rise crops such as cereals or lettuce. This circumstance could be of great interest in countries where agriculture is one of the fundamental economic activities. In addition, in recent times, the number of large areas of land dedicated to PV installations connected to the grid is growing, highlighting among them the installations with solar trackers on a horizontal N–S axis. Thus, the introduction of agrivoltaics by combining these large PV facilities with N–S tracking with tree crops, such as olive groves or citrus, planted in hedgerows in the lanes between solar trackers, would result in a positive contribution to a more modern, sustainable, and efficient agricultural model.

However, these tree crops could partially shade the solar collectors, negatively affecting PV production. Moreover, the shading of the panels can lead to production losses of up to 70% [27,28] since the levels of solar irradiance incident on the collectors are reduced by not receiving their direct component. In addition, shaded solar cells become hot spots that consume the energy of neighbouring cells, increasing their temperature [29].

As a solution to the partial shading of solar collectors, when this is due to the interaction between consecutive rows of panels in PV plants with solar trackers, different authors have proposed tracking/backtracking strategies to eliminate such shading [30–38]. To do this, at times of intershading between PV modules, backtracking proposes to vary the inclination of the modules until the shadow of each row of modules does not affect the rear row.

In a similar way, when considering the conversion of PV plants into agrivoltaic plants with crops in a hedge between the rows of solar collectors, it is necessary to analyse the shadows that the crop can cast on these PV panels since it could affect energy production. However, no works aimed at characterising this behaviour have been found in the literature. In this context, the present work analyses a novel proposal for an agrivoltaic plant based on the cultivation of hedgerow trees between the rows of an existing PV plant with horizontal trackers on a N–S axis. Furthermore, this research presents a new tracking strategy that improves the yield of these plants by eliminating the possible shadows of the crop on the PV panels. For this purpose, the behaviour of the solar irradiance in the agrivoltaic facility proposed is modelled and the shading of the crop

on the PV panels is simulated. From the results of this simulation, a geometric space between the rows of solar collectors available for crops without affecting the irradiance capture or the tracking strategy has been identified (sections 2.1 and 2.2). Subsequently, section 2.3 analyses how the tracking/backtracking strategy of the collectors should be modified when the crops exceed the non-influence region previously mentioned. Finally, section 2.4 presents the methodology to characterise the solar radiation on PV collectors obtained when the solar trackers of the agrivoltaic plant move according to the modified tracking/backtracking strategy proposed as a novelty in this work. Therefore, this research contributes to the progress of knowledge in the field of agrivoltaics while promoting a sustainable and efficient agricultural model.

## 2. Methodology

The PV plants with N–S axis horizontal trackers show simple geometric characteristics as represented in Fig. 1.

The action of conversion to agrivoltaics studied in this work consists of the implantation of a line of crops in the central area of the lanes between trackers. For the geometric characterisation of the crop, it is considered that, whatever the actual shape of the tree, it will not exceed the limits of a rectangle of height  $h_c$  and width  $a_c$  (Fig. 2).

In both figures the horizontal reference system is considered in which the axis Ox is oriented towards the west and the axis Oy towards the south and the axis Oz towards the zenith. In this way, the projection of the crop on the Oxz plane would be contained in the rectangle of dimensions  $a_c$  and  $h_c$  in correspondence with the agronomic description of hedge crops.

### 2.1. Astronomical considerations

For the analysis of intershading between collectors and the corresponding tracking/backtracking strategy that is proposed in this work, it is necessary to simulate the incidence of solar radiation in the plant under study. To do this, the vector description is used both for the positioning of the sun in the sky and to describe the orientation of the solar collectors.

Letting  $\vec{i}$ ,  $\vec{j}$  and  $\vec{k}$  be the unit vectors on the axes Ox, Oy and Oz, respectively, of the horizontal reference system described above, the solar vector,  $\vec{s}$ , will be expressed by Eq. (1), in which  $\psi$  is the latitude of the place,  $\Omega = \frac{\pi}{12} \text{ rad/h}$  is the angular speed of rotation of the Earth,  $t$  is the solar hour and  $\delta$  is the declination.

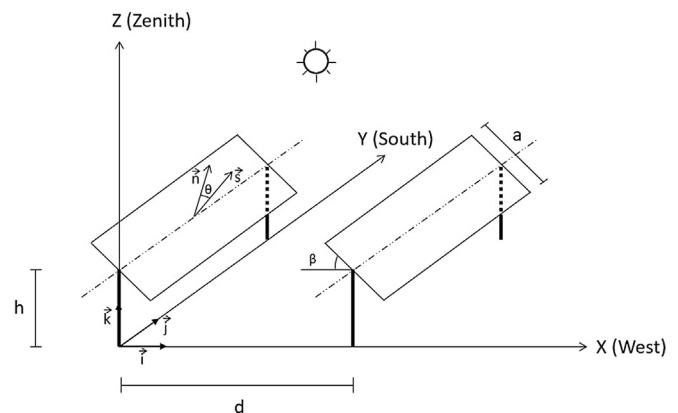


Fig. 1. Representation of a PV plant with N–S axis tracking.

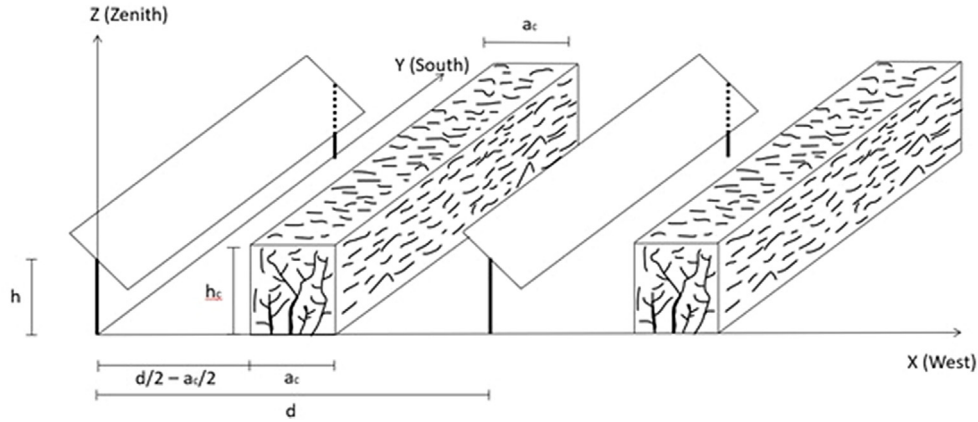


Fig. 2. Representation of an agrivoltaic plant tracking with N–S axis and crops in lines.

$$\begin{aligned} \vec{s} &= s_x \vec{i} + s_y \vec{j} + s_z \vec{k} \\ &= (\sin \Omega t \cdot \cos \delta) \vec{i} + (\cos \Omega t \cdot \cos \delta \cdot \sin \psi - \sin \delta \cdot \cos \psi) \vec{j} \\ &\quad + (\cos \Omega t \cdot \cos \delta \cdot \cos \psi + \sin \delta \cdot \sin \psi) \vec{k} \end{aligned} \tag{1}$$

According to the model proposed by Spencer [39], the declination  $\delta$  depends on the Julian day  $d_j$  using Eqs. (2) and (3).

$$\begin{aligned} \delta(\text{rad}) &= [0.006918 - 0.399912 \cos(\Gamma) + 0.070257 \sin(\Gamma) \\ &\quad - 0.006758 \cos(2\Gamma) + 0.000907 \sin(2\Gamma) \\ &\quad - 0.002697 \cos(3\Gamma) + 0.00148 \sin(3\Gamma)] \end{aligned} \tag{2}$$

$$\Gamma(\text{rad}) = \frac{2\pi(d_j - 1)}{365} \tag{3}$$

2.2. Tracking and backtracking in a PV plant with an N–S axis without crops

First, as a point of reference, a PV plant with N–S horizontal single-axis solar trackers is considered. Usually, these facilities carry out astronomical solar tracking, which, at every moment, seeks to minimise the solar incidence angle  $\theta$ , which forms the solar vector  $\vec{s}$  with the normal vector to the collectors,  $\vec{n}$ . This condition is expressed by Eq. (4).

$$\vec{n} = \frac{s_x}{\sqrt{s_x^2 + s_z^2}} \vec{i} + \frac{s_z}{\sqrt{s_x^2 + s_z^2}} \vec{k} \tag{4}$$

Fig. 3 shows the view of these PV plants projected on the Oxz plane. From this figure, the apparent solar elevation,  $\gamma$ , can be defined as the angle formed by the projection of the solar vector,  $\vec{s}$ , in the Oxz plane with the Ox axis. According to this definition,  $\gamma$  will be given by Eq. (5).

$$\gamma = \arctg\left(\frac{s_z}{|s_x|}\right) \tag{5}$$

From the apparent solar elevation, the inclination of the collectors at each instant is given by Eq. (6)

$$\beta = \frac{\pi}{2} - \gamma \tag{6}$$

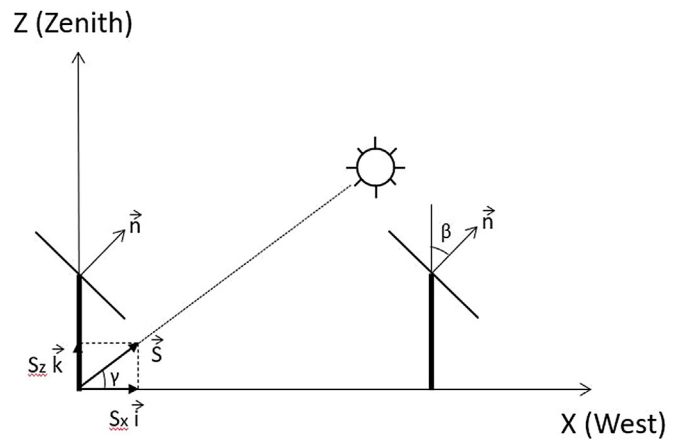


Fig. 3. Graphic representation in the Oxz plane of a PV plant with tracking to an N–S axis and the apparent solar height.

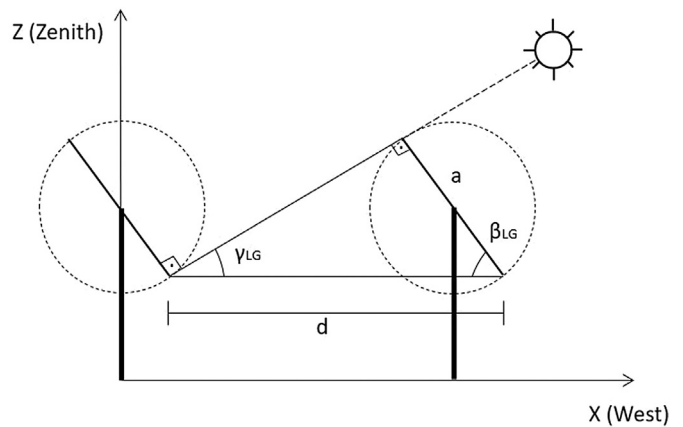


Fig. 4. Limit situation between astronomical tracking and backtracking for a PV plant with tracking on an N–S axis.

However, this movement in the early and late hours of the day, when the sun’s rays strike at low solar height, generate inter-shading of collectors, which leads to significant negative effects on the operation of the PV plant [29,40–43]. In accordance with this, to avoid this intershading between panels, different authors propose the backtracking or movement strategy that disorients the

collectors with respect to the solar direction, with the aim of eliminating intershading [31,32,37,44]. This movement forces the solar collectors to move closer to the horizontal position at the beginning and end of the day.

Fig. 4 shows the graphical representation of two contiguous rows of collectors in the limit situation in which there is no intershading. For clarity, the circumference described by the ends of the PV collectors in their solar tracking motion has been drawn. From Fig. 4 it is possible to define an apparent solar height limit,  $\gamma_{LG}$ , which corresponds to the common tangent to both circumferences and which, therefore, is given by Eq. (7). Associated with this apparent solar height limit, the limit inclination  $\beta_{LG}$  can be defined as the maximum inclination of the panels for which the astronomical tracking does not imply intershading (Eq. (8)). Both magnitudes depend on geometric and astronomical factors.

$$\gamma_{LG} = \arcsin\left(\frac{a}{d}\right) \tag{7}$$

$$\beta_{LG} = \frac{\pi}{2} - \arcsin\left(\frac{a}{d}\right) \tag{8}$$

Thus, when  $\gamma \geq \gamma_{LG}$  and  $\beta \leq \beta_{LG}$  there is no intershading and the collectors move according to the astronomical tracking strategy. Therefore, the inclination of the panels will be determined by Eqs. (5) and (6), as explained previously. On the contrary, if  $\gamma < \gamma_{LG}$  and  $\beta > \beta_{LG}$ , it is necessary to resort to backtracking to avoid intershading between panels. In this case of back-tracking, the inclination of the collectors  $\beta$  will be given by Eq. (9), as demonstrated in Appendix A.

$$\beta = \frac{\pi}{2} - \gamma - \arcsin\left(\frac{d}{a} \sin \gamma\right) \tag{9}$$

Fig. 5 shows a generic instant in which the solar rays hit with an apparent height lower than  $\gamma_{LG}$ . Consequently, in this situation backtracking is proposed to avoid intershading and the inclination of the panels would be rectified approaching the horizontal. In this position, it is observed that the points  $P$  and  $T$  of the limit ray that passes through the ends of two contiguous collectors have coordinates in the  $Oxz$  plane  $P \equiv \left(\frac{a}{2} \cos \beta, h - \frac{a}{2} \sin \beta\right)$  and  $T \equiv \left(d - \frac{a}{2} \cos \beta, h + \frac{a}{2} \sin \beta\right)$ . Therefore, it is verified that the midpoint  $M$  of this type of rays is a fixed and invariable point, with coordinates  $M \equiv \left(\frac{d}{2}, h\right)$ , that is, it is the midpoint between the axis of the solar collectors. From this reasoning it follows that there is a region  $R$  through

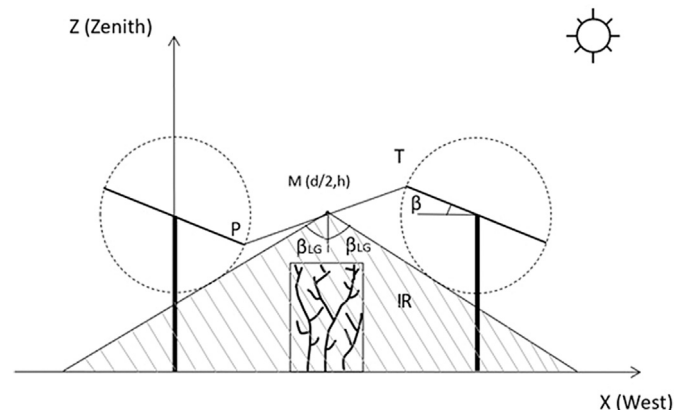


Fig. 5. Representation of the region without direct solar radiation in a PV plant with tracking on an N-S axis.

which in no case do the direct solar rays incident on the collectors. Fig. 5 shows the representation of this region on the  $Oxz$  plane. As a consequence, no crop located in the  $R$  region without exceeding its limits would shade the panels and, therefore, would not affect the tracking/backtracking strategy of the previous PV installation.

However, in commercial trackers it is usual that the inclination of the panels cannot reach the value of  $\beta_{LG}$  since it is limited by the mechanical design. Thus, there is frequently a technological inclination limit value,  $\beta_{LT}$ , that the mechanism cannot exceed. Under these conditions, the value obtained in Eq. (9) must be recalculated with the criteria given by Eq. (10). Furthermore, in the event of this mechanical limit to the inclination of collectors, the  $R$  region would be of greater amplitude than that previously described, as shown in Fig. 6.

$$\text{if } |\beta| > \beta_{LT} \rightarrow \beta = \text{sign}(\beta) \cdot \beta_{LT} \tag{10}$$

### 2.3. Tracking and backtracking in a PV plant with an N-S axis with crops

In this section, the appearance of possible shading when the crop exceeds the non-shading zone  $R$  is analysed. Moreover, a solar tracking strategy is proposed to prevent partial shading of collectors, thus allowing the collectors to always receive a uniform incidence of direct irradiance.

Fig. 7 represents the PV plant with N-S horizontal single-axis

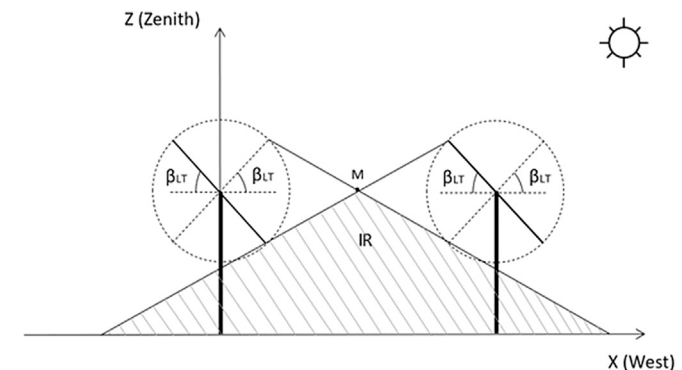


Fig. 6. Influence of the technological limits of inclination of the collectors in the  $R$  region for a PV plant with tracking on an N-S axis.

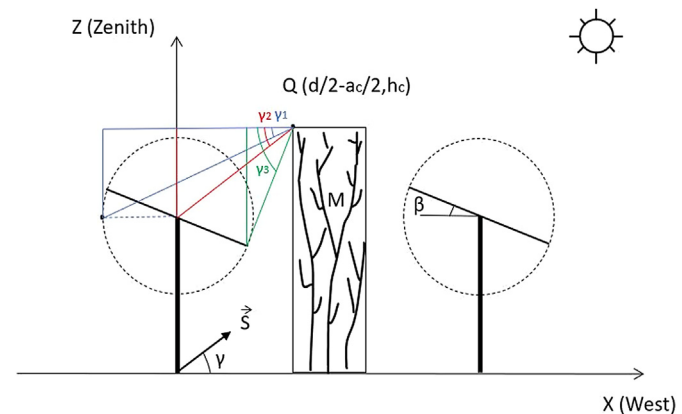


Fig. 7. Geometric representation of the angular limits  $\gamma_1$  (solar collector totally shaded),  $\gamma_2$  (solar collector partially shaded) and  $\gamma_3$  (solar collector no shaded) for the study of crop shading on PV panels.

solar trackers and a crop of dimensions  $a_c$  (width) and  $h_c$  (height) centred at the average distance between two consecutive rows of PV panels. In this figure, according to the tracking/backtracking strategy described in section 2.2 and depending on the apparent solar height, the panels are inclined an angle  $\beta$  which will be given by Eq. (6), in the case of astronomical tracking, or by Eq. (9), in the case of backtracking. In this way, from the analysis of shadows of the crop on the panels, a tracking/backtracking algorithm will be proposed. For it, a corrected tilt value of the panels,  $\beta_c$ , will be provided to avoid the shadows of the crop on the panels. From it, it is possible to calculate the normal vector to the collector  $\vec{n}$  using Eq. (11).

$$\vec{n} = \sin \beta_c \vec{i} + \cos \beta_c \vec{j} \tag{11}$$

To analyse whether the crop produces shading on the panels, the upper left vertex  $Q$  of coordinates  $Q \equiv \left(\frac{d}{2} - \frac{a_c}{2}, h_c\right)$  is considered as the limit situation from which these shadows would be produced. In this way, the algorithm is based on the definition of three delimiting angles for the apparent solar elevation values:

- a)  $\gamma_1$ , when the whole collector is shaded by the crop, given by Eq. (12)
- b)  $\gamma_2$ , when the collector is partially shaded, given by Eq. (13), and
- c)  $\gamma_3$ , when the collector is not shaded, given by Eq. (14) respectively.

$$\gamma_1 = \arctg\left(2 \frac{h_c - h}{d - a_c + a \cdot \cos \beta}\right) \tag{12}$$

$$\gamma_2 = \arctg\left(2 \frac{h_c - h}{d - a_c}\right) \tag{13}$$

$$\gamma_3 = \arctg\left(\frac{2h_c - 2h + a \sin \beta}{d - a_c - a \cos \beta}\right) \tag{14}$$

These delimiting angles define four possible intervals or cases to be considered in the analysis of crop shading on PV panels:

- i)  $0 < \gamma < \gamma_1$ : As long as this condition is met, the collector must remain in a horizontal position without direct irradiance falling on it. Therefore, for this situation,  $\beta_c = 0$  is proposed. Thus, substituting this value in Eq. (11), it is established that the normal vector to the collectors must point to the zenith of the place (Eq. (15))

$$\vec{n} = \vec{k} \tag{15}$$

- ii)  $\gamma_1 < \gamma < \gamma_2$ : In the instants in which this condition occurs, only a part of the collector can access direct irradiance, producing shadows in the rest. In order to avoid partial shading, it has been decided to reorient the collector so as to prevent direct irradiance on it. As demonstrated in Appendix A, the geometric analysis in this hypothesis leads to the Eq. (16) for the corrected inclination of the collectors in which  $D$  is the distance from the vertex  $Q$  to the collector axis given by Eq. (17).

$$\beta_c = \frac{\pi}{2} - \gamma - \arccos\left(\frac{2D}{a} \sin(\gamma_2 - \gamma)\right) \tag{16}$$

$$D = \sqrt{\left(\frac{d}{2} - \frac{a_c}{2}\right)^2 + (h_c - h)^2} \tag{17}$$

- iii)  $\gamma_2 < \gamma < \gamma_3$ : Under these conditions, if the value of  $\beta$  obtained in section 2.2 is maintained, the lower part of the collector would be shaded. However, the correction to the value given by (18) allows uniform access of the direct irradiance to the entire collector, as demonstrated in Appendix A.

$$\beta_c = \frac{\pi}{2} - \gamma - \arccos\left(\frac{2D}{a} \sin(\gamma - \gamma_2)\right) \tag{18}$$

- iv)  $\gamma > \gamma_3$ : In this case, the crop would not shade the collectors. Consequently, it is not necessary to correct the tilt of the collectors.

#### 2.4. Determination of irradiance and solar radiation on PV collectors

Once the tracking/backtracking strategy has been defined for the agrivoltaic plant with N–S horizontal single-axis solar trackers and a crop characterised by a rectangle of width  $a_c$  and height  $d$ , the energy production in this plant is analysed. For this, the incident irradiance on the collectors,  $I$ , is evaluated by means of the sum of its three components (direct, diffuse and reflected), considering three radiative models: Liu–Jordan isotropic model, Hay–Davies anisotropic model and Perez’s anisotropic model.

- a. Isotropic sky model: This model, proposed by Duffie and Beckman [45] and Liu and Jordan [46] assumes that the diffuse component of solar irradiance is isotropically distributed in the celestial sphere. Accordingly, the model establishes that the solar irradiance,  $I$ , is calculated from the direct ( $I_B$ ) and diffuse ( $I_D$ ) solar irradiance on the horizontal surface by means of Eq. (19). In this equation,  $\theta$  is the angle formed by the solar vector and the normal to the collection surface,  $\theta_z$  is the zenith angle and  $\rho$  is the albedo of the reflecting surface.

$$I = \frac{\cos \theta}{\cos \theta_z} I_B + \frac{1 + \cos \beta}{2} I_D + \rho \frac{1 - \cos \beta}{2} (I_B + I_D) \tag{19}$$

- b. Hay–Davies model [47]: it establishes that a certain fraction of the diffuse irradiance, given by the quotient between the direct irradiance on the horizontal surface  $I_B$  and the horizontal extraterrestrial irradiance  $I_{0H}$ ,  $\frac{I_B}{I_{0H}}$ , is directed from the direction of the solar disk. Consequently, it has a behaviour similar to that of the direct component, while the rest of the diffuse irradiance has an isotropic behaviour (Eq. (20)).

$$I = \frac{\cos \theta}{\cos \theta_z} I_B + \left[ \left( \frac{\cos \theta}{\cos \theta_z} \right) \frac{I_B}{I_{0H}} + \left( 1 - \frac{I_B}{I_{0H}} \right) \frac{1 + \cos \beta}{2} \right] I_D + \rho \frac{1 - \cos \beta}{2} (I_B + I_D) \tag{20}$$

- c. Pérez model [48]: Finally, this third model assumes that diffuse irradiance is decomposed, in turn, into three subcomponents: one of an isotropic nature, another from the area near the solar disk and a last one coming from the horizon. Accordingly, the irradiance is given by Eq. (21) in which  $F_1, F_2$  are coefficients that

deliberate the weight of each of the subcomponents of the diffuse irradiance and  $a_p$  and  $b_p$  are given by Eqs. (22) and (23) respectively.

$$I = \frac{\cos \theta}{\cos \theta_z} I_B + \left[ (1 - F_1) \frac{1 + \cos \beta}{2} + F_1 \frac{a_p}{b_p} + F_2 \sin \beta \right] I_D + \rho \frac{1 - \cos \beta}{2} (I_B + I_D) \tag{21}$$

$$a_p = \max(\cos \theta; 0) \tag{22}$$

$$b_p = \max(\cos 85^\circ; \cos \theta_z) \tag{23}$$

Regardless of the model considered, for the instants in which the collectors are shaded,  $\cos \theta = 0$  will be considered in Eqs. (19)–(22). With this, in the irradiance calculation, the direct component and the circumsolar diffuse fraction are eliminated.

For each of these radiative models and the proposed tracking strategy, the incident solar irradiance on solar collectors has been simulated every 3 min in the 12 representative Klein days [49]. From the irradiance, the solar radiation for each of the representative days has been calculated using Eq. (24).

$$H_i = \int_{t \text{ sunrise}}^{t \text{ sunset}} I dt \tag{24}$$

Finally, Eq. (25) allows an estimate of the annual incident radiation on the collecting planes

$$H_y^{est} = \sum_{j=1}^{12} Nd_j \cdot H_j \tag{25}$$

where  $Nd_j$  is the amount of Julian days of the month  $j$ .

### 3. Results and discussion

In this section, the results obtained when applying the exposed methodology to a practical case are presented and discussed. Specifically, a PV plant with N–S horizontal single-axis solar trackers located in Córdoba, Spain (latitude: 37.58° N; Longitude: 4.18° W) with the geometric characteristics shown in Fig. 8 has been chosen for the simulation.

With regard to the crop, four cases of interest have been considered for determining the necessary tracking/backtracking

**Table 1**  
Geometric characteristics of the simulated crop in the agrivoltaic plant.

Case number	$a_{ci}(m)$	$h_{ci}(m)$
0	2	2
1	2	3
2	2	4
3	2	5

**Table 2**  
Daily radiation on the horizontal plane (H) in Córdoba (Spain) taken from Posadillo & López-Luque [50], and representative day considered for each month [49].

Month	H (MJ/m <sup>2</sup> )	Representative day
January	7.401	17
February	11.097	47
March	14.158	75
April	17.307	105
May	19.017	135
June	24.263	162
July	25.719	198
August	23.411	228
September	17.983	258
October	11.895	288
November	8.228	318
December	6.237	344

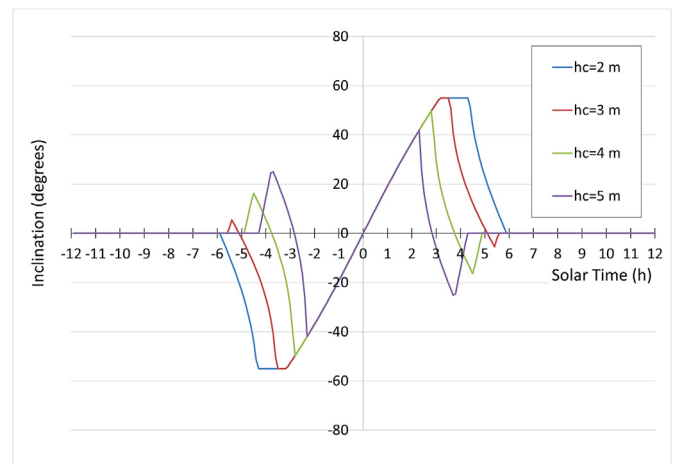


**Fig. 9.** Evolution of the inclination angle  $\beta$  of collectors for four different crop heights.

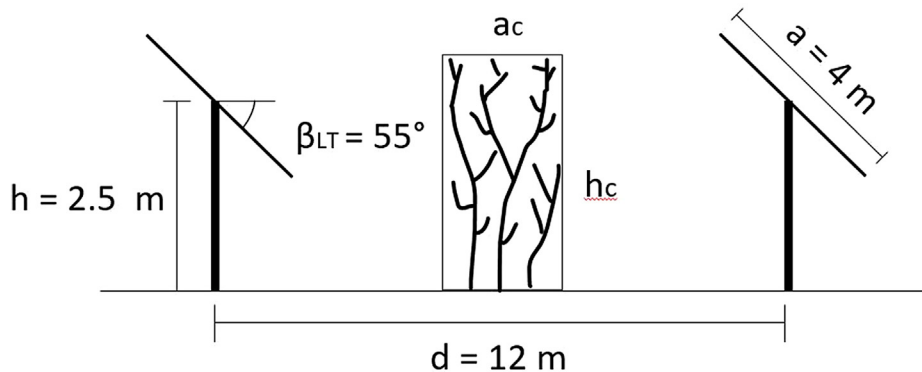


**Fig. 8.** Geometric characteristics of the PV installation considered as a case study.

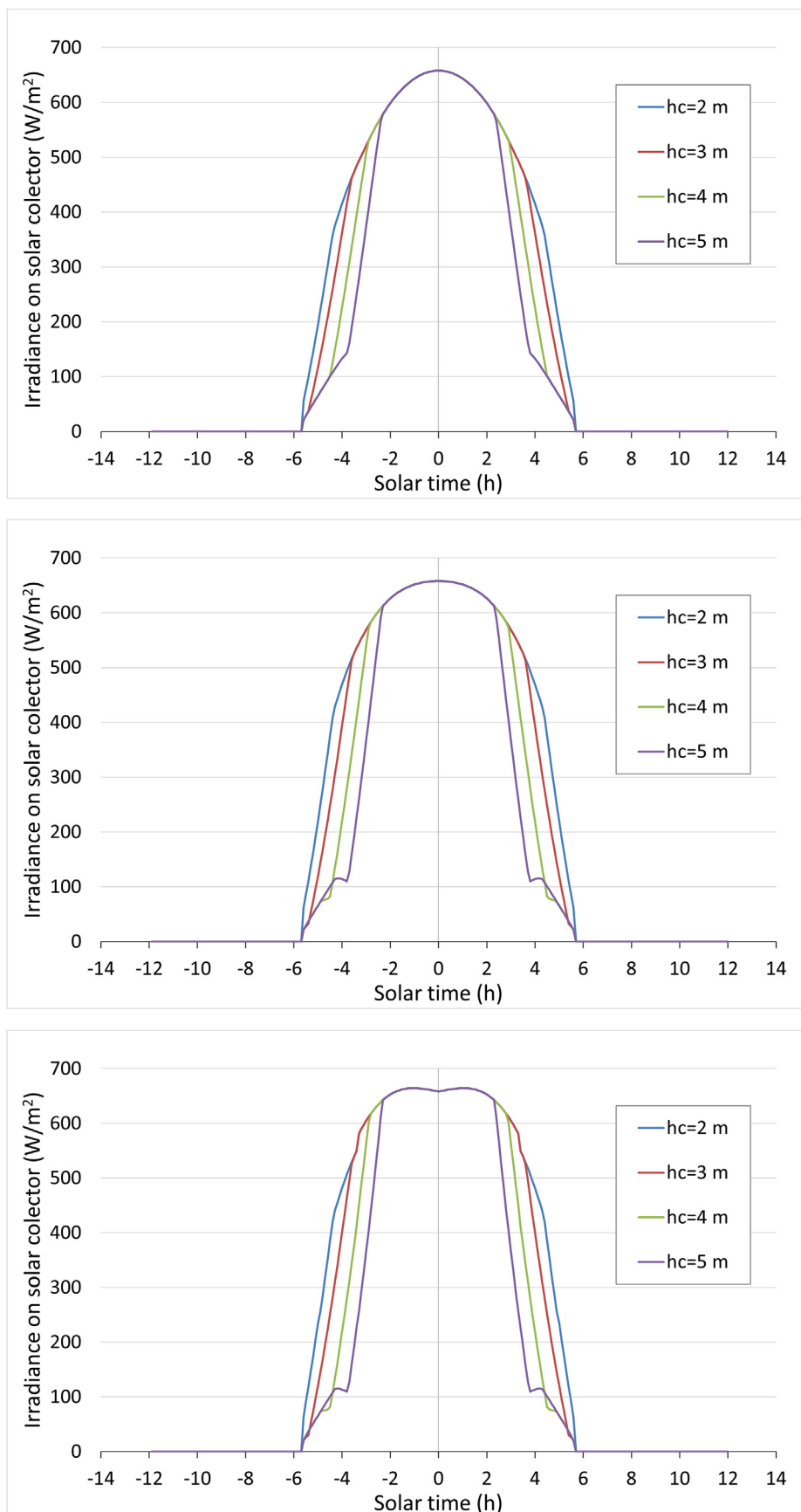


**Fig. 10.** Irradiance on collectors in Córdoba on the representative day of March and depending on the crop heights according to: a) Liu-Jordan model [46]; b) Hay-Davies model [47] and c) Perez model [48].

strategy, as well as for the evaluation of the radiative potential in each case. Although in all cases a fixed width  $a_c = 2\text{ m}$ , has been assumed, the height of the crop has been varied according to the values shown in Table 1. Of the cases considered, the first one ( $a_{c0}$ ,  $h_{c0}$ ) corresponds to a crop that, according to section 2.2, does not interfere with the PV plant monitoring strategy because it is within the R zone. Therefore, it is considered a reference against which to compare the rest of the cases studied ( $a_{c1}$ ,  $h_{c1}$ ), ( $a_{c2}$ ,  $h_{c2}$ ) and ( $a_{c3}$ ,  $h_{c3}$ ).

For each of the cases considered, the application of the methodology set out above allows obtaining the daily evolution of both the position of the collectors and the irradiance incident on them based on the geometric characteristics of the crop. For this, it is necessary to know the values of the representative Julian days of Klein of each month [49], as well as the climatological value of the characteristic solar radiation during this month (Table 2).

Fig. 9 shows the comparison of the tracking strategies for each of the cases planned on the representative day of July (15th July). It shows the different types of tracking in each case, considering the case ( $a_{c0} = 2\text{ m}$ ,  $h_{c0} = 2\text{ m}$ ) as a reference because it gives rise to a tracking policy identical to the previously existing backtracking one. It is observed that, the greater the degree of obstruction, the more it takes to start the daily movement and the earlier the movement ends. It is also appreciated that the curves of the cases with obstruction begin with a rise in the angle  $\beta$  during which the collectors do not receive direct radiation to avoid the partial shading of collectors. For the same reason, they also show a final downward stretch before being horizontal or waiting the next day.

Fig. 10 show the estimated irradiance according to the Liu-Jordan [46], Hay-Davies [47] and Pérez [48] models respectively for the four cases considered and the representative day of the month of March. Among them, there is a high similarity in terms of behaviour. In cases with obstruction, the initial and final sections of the curve correspond to moments in which only the diffuse radiation falls on the collectors that are either horizontal or adapting their position to avoid direct irradiance. There are also sections with high linearity that correspond to the backtracking periods and a central section in which astronomical monitoring is carried out.

For all months it is observed that the isotropic model [46] predicts lower levels of irradiance than the Hay-Davies [47] or Perez [48] models. This is due to the fact that the structure of the anisotropic models separates a fraction of the diffuse irradiance that follows a behaviour analogous to the direct one. This implies that in the simulation with solar trackers, higher capture values are always obtained with the anisotropic models. This effect is also observed when irradiances are compared in the periods in which there is no direct irradiance. The diffuse values decrease in the anisotropic models with respect to the isotropic one.

For the practical quantification of the degree of obstruction according to the irradiance models, the annual profiles have been obtained. For that purpose, the 12 representative days, in the four cases proposed for analysis have been considered. Fig. 11 shows this evolution, evidencing in it that the differences in incident radiation on collectors are higher in summer than in winter months. The differences become greater in the anisotropic models for the reasons previously discussed.

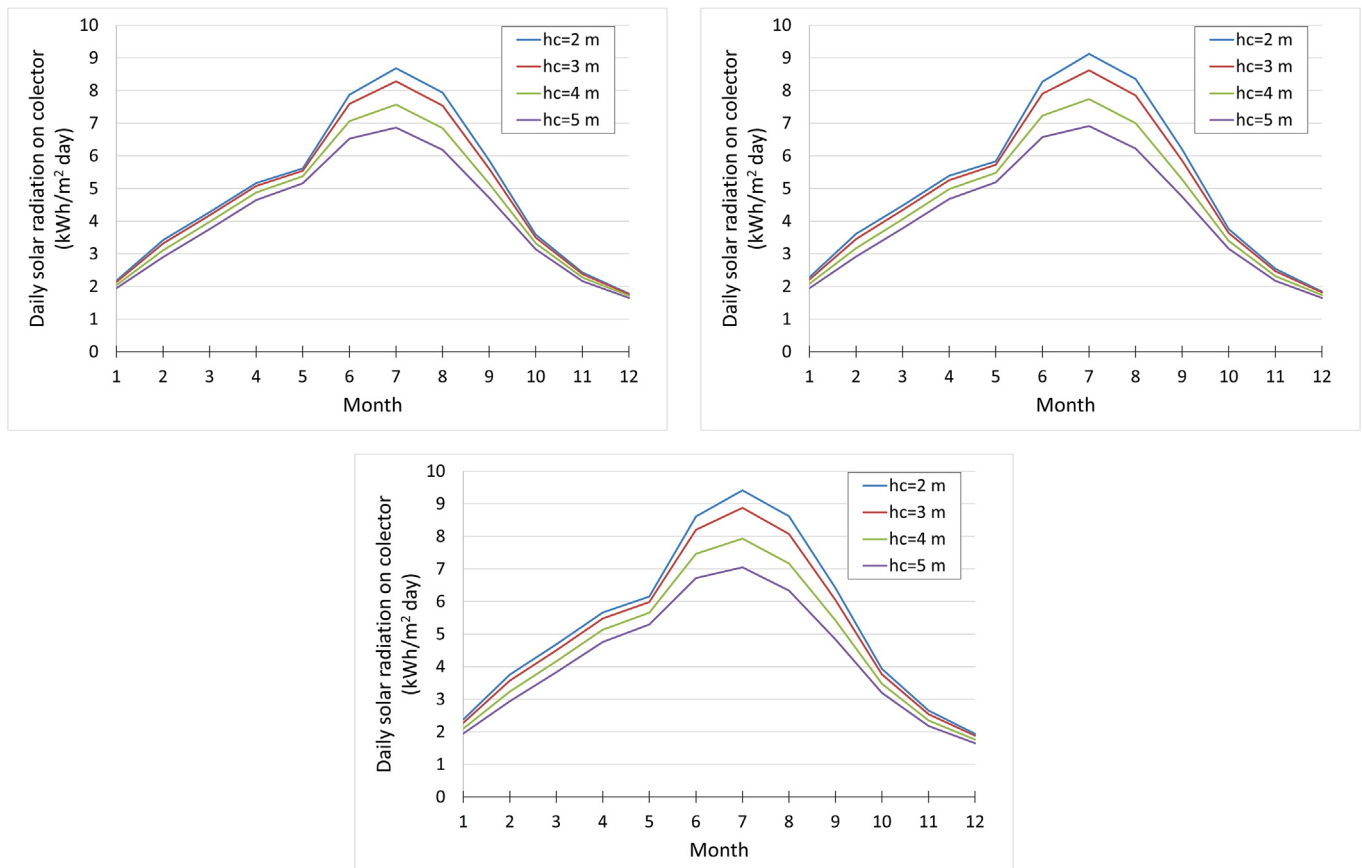


Fig. 11. Incident radiation on collectors estimated according to: (a) Liu-Jordan model [46], (b) Hay -Davies model [47] and (c) Perez model [48].

Thus, Fig. 12 shows, for each of the obstructed cases, the ratio  $r$  which indicates in the radiative decay due to the obstruction (Eq. (26)).

$$r = \frac{H(hc \in R)}{H(hc \notin R)} \tag{26}$$

In general, a higher decay is obtained for all models in the crops with the highest degree of obstruction. When comparing models, it can be seen that the anisotropic ones predict lower ratios than the isotropic one. This is because the geometric character of the shading harms the models that consider the existence of irradiance of diffuse circumsolar origin.

Finally, to delve into the dependence of the annual radiation in the selected standard installation with respect to the dimensions of the crop ( $a_c$ ,  $h_c$ ), as well as to offer graphically a practical result of rapid application, the annual energy losses by varying  $a_c$  between 0 and 3 m and  $h_c$  between 0 and 4 m in the selected installation have been analysed. Fig. 13 shows the representation by level curves of such losses and the position of the Q point on these lines indicates the radiative loss to which the crop gives rise.

The graphs in Fig. 13 allow an estimation of the LER parameter of PV installations converted to agrivoltaic plants. As an example, the LER calculation is presented in the installation obtained by inserting a super-intensive olive grove hedge with  $h_c = 3.0m$  and  $a_c = 1.5m$ , knowing that in a purely agricultural farm this type of hedge would be between 4 m and 6 m apart. According to Dupraz et al. [14], the LER for this example installation would be the sum of the yield ratios of photovoltaic power production and agricultural production (Eq.(27)),

$$LER = \frac{\eta_{PV-AGPG}}{\eta_{PV}} + \frac{\eta_{AG-AGPV}}{\eta_{AG}} \tag{27}$$

where  $\eta_{PV-AGPG}$  and  $\eta_{AG-AGPV}$  are respectively the photovoltaic and agricultural efficiency in the agrivoltaic installation and  $\eta_{PV}$  and  $\eta_{AG}$  are respectively the yields of the land when it is exclusively dedicated to photovoltaic and agricultural production.

To calculate the first of the ratios, it is admitted that the energy production is proportional to the annual radiation incident on the collectors. Likewise, from Fig. 13 three estimates are obtained depending on the radiative model considered. Specifically, for each model, the losses are obtained from the isoline intersected by the rectangle representing the crop in Fig. 13. Thus, the estimates will be given by Eqs. (28)–(30):

$$\left(\frac{\eta_{PV-AGPG}}{\eta_{PV}}\right)_{Iso} = \frac{100 - 2.8}{100} = 0.978 \tag{28}$$

$$\left(\frac{\eta_{PV-AGPG}}{\eta_{PV}}\right)_{H-D} = \frac{100 - 3.6}{100} = 0.964 \tag{29}$$

$$\left(\frac{\eta_{PV-AGPG}}{\eta_{PV}}\right)_{Perez} = \frac{100 - 4.1}{100} = 0.959 \tag{30}$$

Regarding the ratio of agricultural yields, it is considered that the productive drop is proportional to the drop in the density of hedges with respect to the crop in exclusively agricultural conditions [51]. In this way, the values given by Eqs. (31) and (32) are obtained

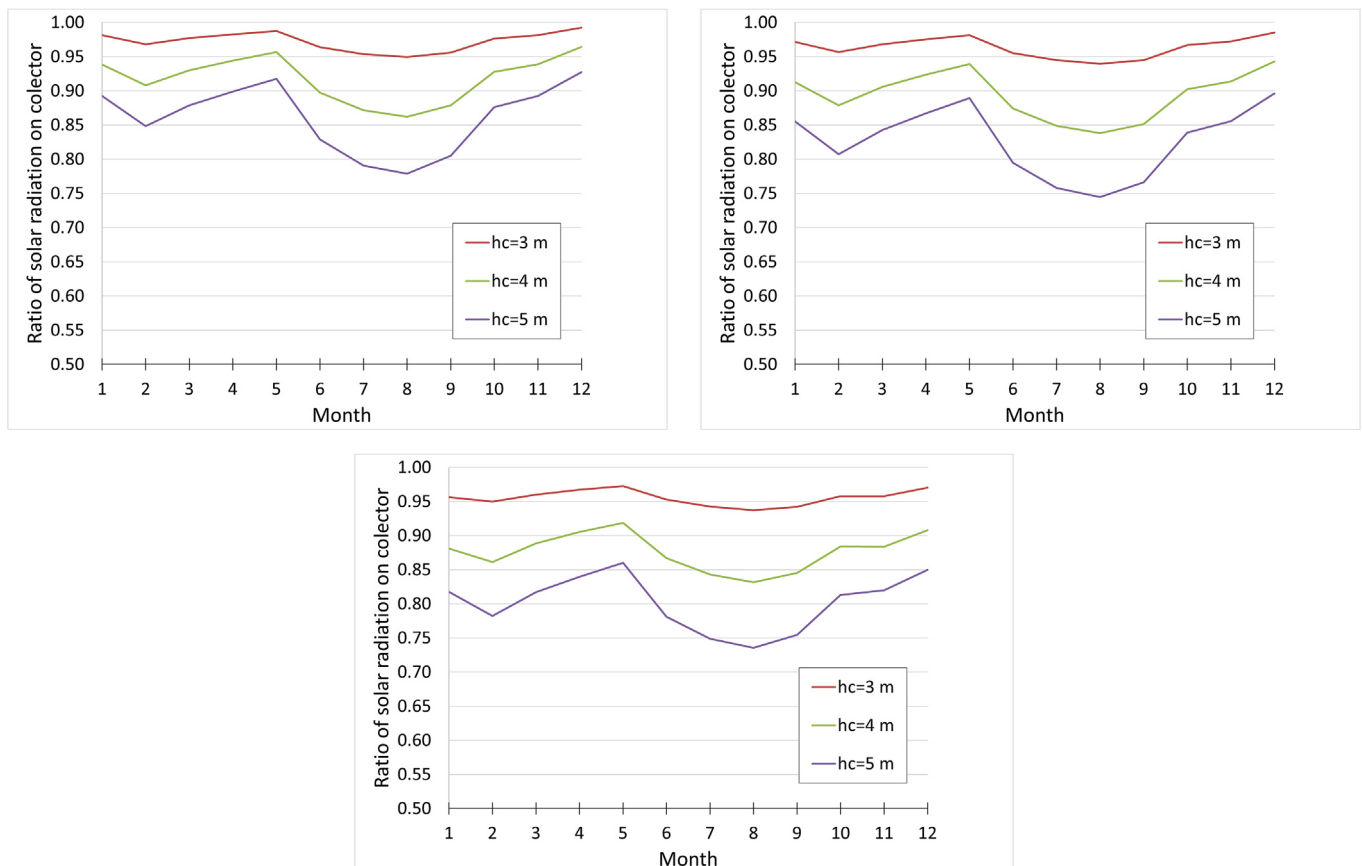


Fig. 12. Radiation decay rate  $r$  on collectors estimated according to: (a) Liu-Jordan model [46], (b) Hay -Davies model [47] and (c) Perez model [48].

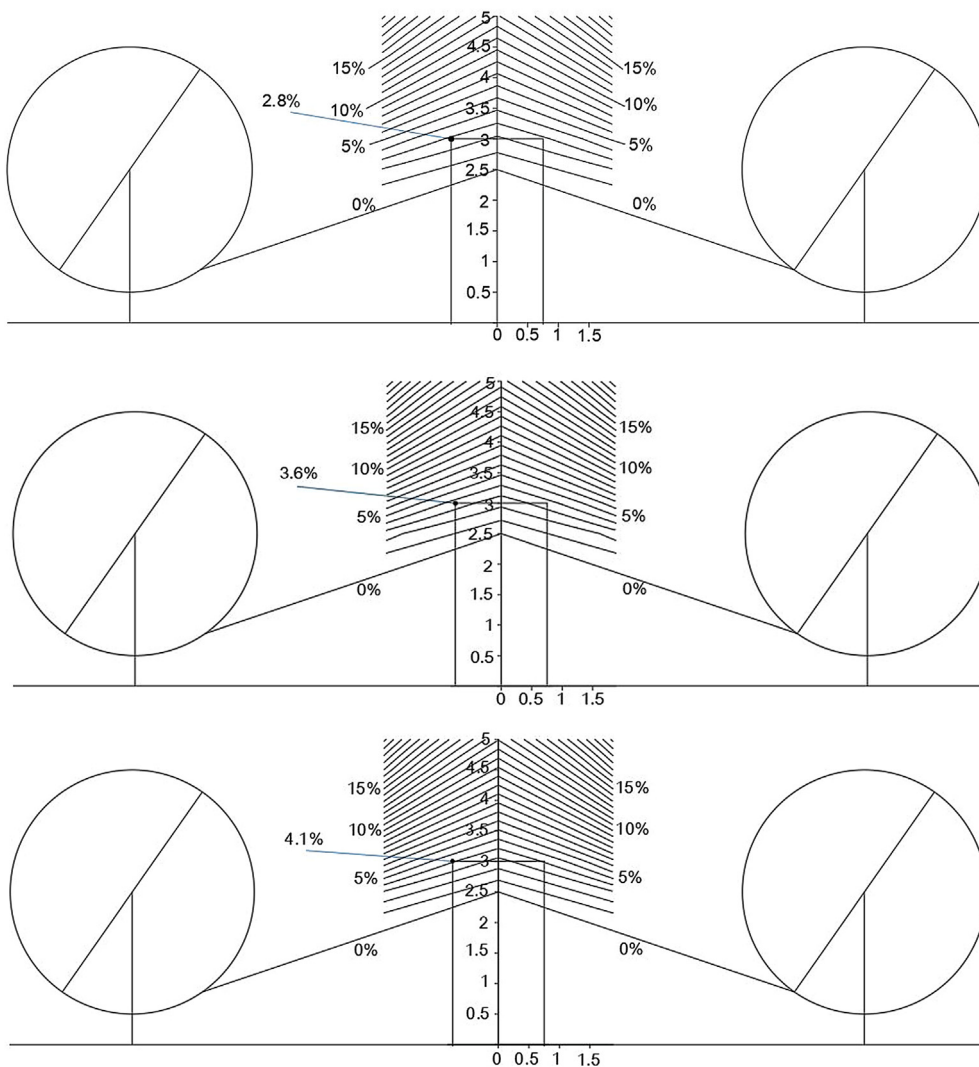


Fig. 13. Annual radiation losses in collectors depending on the position of Q in the isoline field. Here are distinguished the models of: (a) Liu-Jordan model [46], (b) Hay -Davies model [47] and (c) Perez model [48].

$$\left(\frac{\eta_{AG-AGPV}}{\eta_{AG}}\right)_{4\ m} = \frac{1\ (crop\ hedgerow\ every\ 12\ m\ in\ AGPG)}{3\ (crop\ hedgerow\ every\ 12\ m\ in\ AG)} = 0.33 \tag{31}$$

$$\left(\frac{\eta_{AG-AGPV}}{\eta_{AG}}\right)_{6\ m} = \frac{1\ (crop\ hedgerow\ every\ 12\ m\ in\ AGPG)}{2\ (crop\ hedgerow\ every\ 12\ m\ in\ AG)} = 0.5 \tag{32}$$

Table 3 shows the six possible estimates of when combining the results of the yields given by equations (28)–(30), resulting from the different alternatives considered and previously described. This example, in addition to showing the application of the graphs in Fig. 13, allows to verify that, a priori, the productivity of the land in an agrivoltaic installation located in Córdoba (Spain) under the hypotheses and the design conditions considered, will be seen increased between 28.9% and 47.2%.

#### 4. Conclusions

Agrivoltaics proposes combining agricultural production with the photovoltaic technology on the same land. Thus, it is possible to

Table 3

Calculation of the range of variation of the LER for an agrivoltaic plant with N–S horizontal single-axis solar trackers and crop of olive groves in hedge of dimensions  $h_c = 3.0\ m$  and  $a_c = 1.5\ m$

	$\left(\frac{\eta_{AG-AGPV}}{\eta_{AG}}\right)_{4\ m}$	$\left(\frac{\eta_{AG-AGPV}}{\eta_{AG}}\right)_{6\ m}$
$\left(\frac{\eta_{PV-AGPG}}{\eta_{PV}}\right)_{Iso}$	1.302	1.472
$\left(\frac{\eta_{PV-AGPG}}{\eta_{PV}}\right)_{H-D}$	1.294	1.464
$\left(\frac{\eta_{PV-AGPG}}{\eta_{PV}}\right)_{Perez}$	1.289	1.459

optimise the yield of the land and reduce the conflict over the use of land for large PV facilities. This new model has important advantages from the agricultural, economic and energy point of view, such as the water balance of the land, the improve of the production of certain crops, the reduction of financial risk for farmers and the promotion of a more efficient and sustainable energy system. Accordingly, it seems appropriate to promote the implementation of agrivoltaic facilities. To this end, this work presents a novel proposal to take advantage of the growing number of photovoltaic

installations with N–S axis tracking that are being installed to transform them into agrivoltaic plants. Specifically, planting tree crops in hedges between the rows of PV collectors is proposed.

In that line of work, in the present research an in-depth simulation study of the possible shading of crops on photovoltaic panels has been carried out. As a result of this study, it is shown that, under the basic hypotheses established, there is a geometric space of possible use for crops that would not shade the panels and consequently would not affect the photovoltaic production of a pre-existing PV plant (Fig. 6). However, given the possibility of exceeding this region, a new collector tracking/backtracking strategy has been proposed to minimise the effect of partial shading on collectors. The radiation obtained after following these strategies has also been quantified. Specifically, the reduction of the solar radiation reaching the solar collectors when they move according to the tracking/backtracking strategy proposed is represented by means of isolines (Fig. 13). In that way, it is recommended that the manager of any PV plant with N–S solar trackers, following the proposed methodology, obtains the corresponding isolines of radiation losses. Thus, based on this graphic, the PV plant manager can evaluate the convenience of converting a PV plant to an agrivoltaic plant with hedge crops also oriented in the N–S direction. Particularly, in the case of an agrivoltaic plant with N–S horizontal single-axis solar trackers and an olive grove in a hedge of dimensions  $h_c = 3.0\text{ m}$  and  $a_c = 1.5\text{ m}$  located in Córdoba (Spain), it is verified that the LER of the land could increase between 28.9% and 47.2%.

The authors consider the progress achieved in this study to be very significant as the natural evolution of the implementation of PV power plants with single-axis trackers will force, over the coming years, the search for solutions to their conversion to agrivoltaic facilities. However, a campaign of experimental measures is necessary to corroborate the simulated results, as well as to deepen the knowledge of the response of crops to conditions in which radiation would be limited by shared use with photovoltaics.

### Credit author statement

F.J. Casares de la Torre: Methodology; Validation; Investigation; Resources M.Varo-Martinez: Methodology; Formal analysis; Writing – original draft; Funding acquisition R. López-Luque: Conceptualization, Methodology; Software; Supervision J. Ramírez-Faz: Software; Visualization; Resources; Project administration L.M. Fernández-Ahumada: Software; Validation; Data curation; Writing – review & editing.

### Declaration of competing interest

The authors declare that they have no known competing financial interests or personal relationships that could have appeared to influence the work reported in this paper.

### Acknowledgements

The authors would like to thank the University of Córdoba (Spain) for its support and funding by means of “PLAN PROPIO DE INVESTIGACION UCO” (Grant reference: P.P. 2021 Submod. 1.2) as well as for the funding for Open Access publication charges (Funding for open access charge: University of Cordoba / CBUA).

### Appendix A. Deduction of inclination angle as A function of geometry

#### i) Collector inclination during backtracking, $\beta$ (Eq. (9)), in a photovoltaic plant with N–S axis tracking

Fig. A.1 shows the situation of two contiguous rows of trackers of a photovoltaic plant with N–S horizontal single-axis solar tracking at a time when backtracking is performed. In it, the triangle  $MP_2C$  with sides  $MC = d/2$  and  $CP_2 = a/2$  is considered. Applying the sine theorem, it is obtained that the angle  $\alpha \equiv \widehat{MP_2C}$ , corresponding to the vertex  $P_2$ , is given by Eq. (A.1).

$$\alpha = \arcsin\left(\frac{d}{a} \sin \gamma\right) \tag{A.1}$$

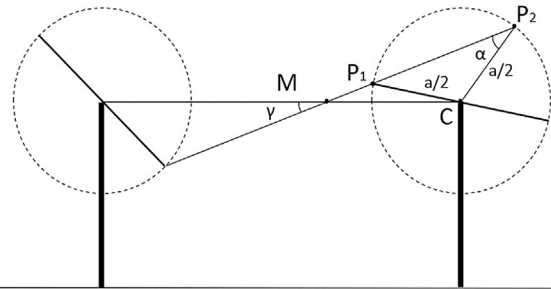


Fig. A.1. Representation of two contiguous rows of PV panels during backtracking in a PV plant with N–S horizontal single-axis solar trackers.

Furthermore, from Fig. A.1, it is observed that the angle  $\widehat{MP_1C}$  verifies Eq. (A.2).

$$\widehat{MP_1C} = \pi - \alpha \tag{A.2}$$

Likewise, for the triangle of vertices  $M$ ,  $P_1$  and  $C$ , Eq. (A.3) is verified.

$$\widehat{MP_1C} + \widehat{CMP_1} + \widehat{P_1CM} = \pi \tag{A.3}$$

Thus, by substituting Eq. (A.2) for Eq. (A.3) and taking into account that, according to Fig. A.1,  $\widehat{CMP_1} = \gamma$  and  $\widehat{P_1CM} = \beta$ , Eq. (A.4) is obtained.

$$(\pi - \alpha) + \gamma + \beta = \pi \tag{A.4}$$

Therefore, isolating  $\beta$  from Eq. (A.4) and considering Eq. (A.5), the Eq. (A.6) that represents the inclination of the collectors during backtracking,  $\beta$ , is obtained. This Eq. (A.6) coincides with Eq. (9) of section 2 of this article.

$$\arcsin \alpha + \arccos \alpha = \frac{\pi}{2} \tag{A.5}$$

$$\beta = \frac{\pi}{2} - \gamma - \arcsin\left(\frac{d}{a} \sin \gamma\right) \tag{A.6}$$

#### ii) Corrected inclination of the collectors during backtracking, $\beta_c$ (Eq. (16)), in an agrivoltaic plant with solar trackers to a N–S axis and crops in hedgerows in the case in which $\gamma_1 < \gamma < \gamma_2$

Fig. A.2 shows the rotation of a solar tracker in a PV plant with N–S horizontal single-axis tracking transformed into an agrivoltaic plant with a hedgerow crop at a time of backtracking in which  $\gamma_1 < \gamma < \gamma_2$ . In that situation, the collector may not be fully exposed to sunlight. Under these conditions it is necessary to position it so that direct irradiance does not affect it. Applying the sine theorem to triangle  $PCQ$ , Eq. (A.7) for the angle  $\alpha$  is obtained.

$$\alpha = \arcsin\left(\frac{2D}{a} \sin(\gamma_2 - \gamma)\right) \tag{A.7}$$

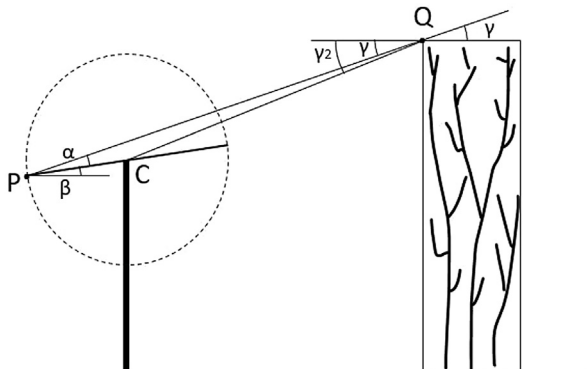


Fig. A.2. Representation of the influence of a hedgerow crop on an agrivoltaic plant with solar trackers on a N–S axis in the case of backtracking where  $\gamma_1 < \gamma < \gamma_2$ .

Furthermore, the inclination angles of the lines starting from P verify Eq. (A.8). In this way, solving for  $\beta_c$  from (A.8) and substituting the relationship between the arcsine and arc cosine functions (Eq. (A.5)), as well as Eq. (A.7), the Eq. (A.9) is obtained. This Eq. (A.9) coincides with Eq. (16) of the article which represents the corrected inclination of the collectors during backtracking in an agrivoltaic plant with N–S horizontal single-axis solar trackers and hedgerow crop in the case in which  $\gamma_1 < \gamma < \gamma_2$

$$\alpha + (-\beta_c) = \gamma \tag{A.8}$$

$$\beta_c = \frac{\pi}{2} - \gamma - \arccos\left(\frac{2D}{a} \sin(\gamma_2 - \gamma)\right) \tag{A.9}$$

ii) Corrected inclination of the collectors during backtracking,  $\beta_c$  (Eq. (18)), in an agrivoltaic plant with solar trackers to a N–S axis and hedgerow crop in the case in which  $\gamma_2 < \gamma < \gamma_3$

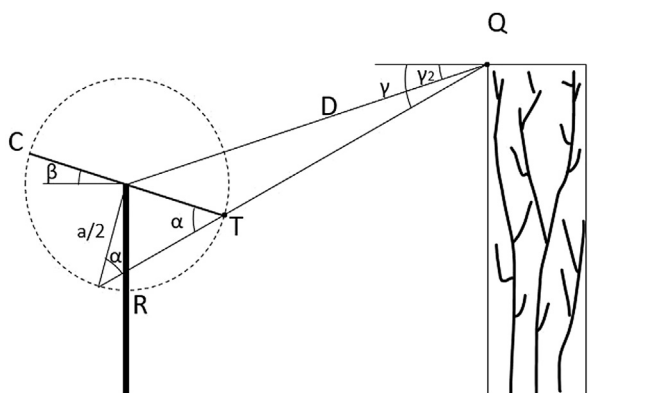


Fig. A.3. Representation of the influence of a hedgerow crop on an agrivoltaic plant with solar trackers on a N–S axis in the case of backtracking where  $\gamma_2 < \gamma < \gamma_3$ .

Fig. A.3 shows the rotation of a solar tracker in a PV plant with N–S horizontal single-axis solar tracking transformed into an agrivoltaic plant with hedgerow crop at a time of backtracking in which  $\gamma_2 < \gamma < \gamma_3$ . In this situation, to avoid the shadow of Q on the collector, it must be rotated so that this shadow coincides with the

end T of the collector. Applying the sine theorem to the triangle RCQ, Eq. (A.10) for the angle  $\alpha$  is obtained.

$$\alpha = \arcsin\left(\frac{2D}{a} \sin(\gamma_1 - \gamma_2)\right) \tag{A.10}$$

Furthermore, from Fig. A.3, it is observed that the angle  $\widehat{CTQ}$  verifies Eq. (A.11).

$$\widehat{CTQ} = \pi - \alpha \tag{A.11}$$

Likewise, for the triangle of vertices C, T and Q, Eq. (A.12) is verified.

$$\widehat{CTQ} + \widehat{QCT} + \widehat{TQC} = \pi \tag{A.12}$$

Thus, by substituting Eq. (A.11) in Eq. (A.12) and taking into account that, according to Fig. A.3,  $\widehat{QCT} = \gamma_2 + \beta$  and  $\widehat{TQC} = \gamma - \gamma_2$ , Eq. (A.13) is obtained.

$$(\pi - \alpha) + (\gamma_2 + \beta_c) + (\gamma - \gamma_2) = \pi \tag{A.13}$$

Therefore, isolating  $\beta$  from Eq. (A.13) and considering Eq. (A.5), the Eq. (A.14) is obtained. This Eq. (A.14) coincides with Eq. (18) of the article which representing the corrected inclination of the collectors during backtracking in an agrivoltaic plant with N–S horizontal single-axis solar trackers and hedgerow crop in the case where  $\gamma_2 < \gamma < \gamma_3$

$$\beta_c = \frac{\pi}{2} - \gamma - \arccos\left(\frac{2D}{a} \sin(\gamma - \gamma_2)\right) \tag{A.14}$$

### References

- [1] Department of Economic and Social Affairs of United Nations, World population prospects 2019. <https://population.un.org/wpp/>, 2019. (Accessed 17 December 2021).
- [2] S. Amaducci, X. Yin, M. Colauzzi, Agrivoltaic systems to optimise land use for electric energy production, *Appl. Energy* 220 (2018) 545–561, <https://doi.org/10.1016/j.apenergy.2018.03.081>.
- [3] International Energy Agency -IEA, Electricity market report - July 2021. <https://www.iea.org/reports/electricity-market-report-july-2021>, 2021. (Accessed 17 December 2021).
- [4] G. Kavlak, J. McNerney, J.E. Trancik, Evaluating the causes of cost reduction in photovoltaic modules, *Energy Pol.* 123 (2018) 700–710, <https://doi.org/10.1016/j.enpol.2018.08.015>.
- [5] M. Victoria, N. Haegel, I.M. Peters, R. Sinton, A. Jäger-Waldau, C. del Cañizo, C. Breyer, M. Stocks, A. Blakers, I. Kaizuka, K. Komoto, A. Smets, Solar photovoltaics is ready to power a sustainable future, *Joule* 5 (2021) 1041–1056, <https://doi.org/10.1016/j.joule.2021.03.005>.
- [6] IEA photovoltaic power systems programme, snapshot of global PV markets 2021. [https://iea-pvps.org/wp-content/uploads/2021/04/IEA\\_PVPS\\_Snapshot\\_2021-V3.pdf](https://iea-pvps.org/wp-content/uploads/2021/04/IEA_PVPS_Snapshot_2021-V3.pdf), 2021.
- [7] International Energy Agency -IEA, Renewables 2020, Paris. <https://www.iea.org/reports/renewables-2020>, 2020.
- [8] S. Nonhebel, Renewable energy and food supply: will there be enough land? *Renew. Sustain. Energy Rev.* 9 (2005) 191–201, <https://doi.org/10.1016/j.rser.2004.02.003>.
- [9] A. Weselek, A. Ehmann, S. Zikeli, I. Lewandowski, S. Schindele, P. Högy, Agrophotovoltaic systems: applications, challenges, and opportunities. A review, *Agron. Sustain. Dev.* 39 (2019), <https://doi.org/10.1007/S13593-019-0581-3/FIGURES/1>.
- [10] A. Goetzberger, A. Zastrow, On the coexistence of solar-energy conversion and plant cultivation, *Int. J. Sol. Energy* 1 (1982) 55–69, <https://doi.org/10.1080/01425918208909875>.
- [11] A. Agostini, M. Colauzzi, S. Amaducci, Innovative agrivoltaic systems to produce sustainable energy: an economic and environmental assessment, *Appl. Energy* 281 (2021).
- [12] B. Valle, T. Simonneau, F. Sourd, P. Pechier, P. Hamard, T. Frisson, M. Ryckewaert, A. Christophe, Increasing the total productivity of a land by combining mobile photovoltaic panels and food crops, *Appl. Energy* 206 (2017) 1495–1507, <https://doi.org/10.1016/j.apenergy.2017.09.113>.
- [13] H. Dinesh, J.M. Pearce, The potential of agrivoltaic systems, *Renew. Sustain. Energy Rev.* 54 (2016) 299–308, <https://doi.org/10.1016/j.rser.2015.10.024>.

- [14] C. Dupraz, H. Marrou, G. Talbot, L. Dufour, A. Nogier, Y. Ferard, Combining solar photovoltaic panels and food crops for optimising land use: towards new agrivoltaic schemes, *Renew. Energy* 36 (2011) 2725–2732, <https://doi.org/10.1016/j.renene.2011.03.005>.
- [15] N. Irie, N. Kawahara, A.M. Esteves, Sector-wide social impact scoping of agrivoltaic systems: a case study in Japan, *Renew. Energy* 139 (2019) 1463–1476, <https://doi.org/10.1016/j.renene.2019.02.048>.
- [16] A. Leon, K.N. Ishihara, Assessment of new functional units for agrivoltaic systems, *J. Environ. Manag.* 226 (2018) 493–498, <https://doi.org/10.1016/j.jenvman.2018.08.013>.
- [17] D. Majumdar, M.J. Pasqualetti, Dual use of agricultural land: introducing 'agrivoltaics' in phoenix metropolitan statistical area, USA, *Landsc. Urban Plann.* 170 (2018) 150–168, <https://doi.org/10.1016/j.landurbplan.2017.10.011>.
- [18] H. Marrou, J. Wery, L. Dufour, C. Dupraz, Productivity and radiation use efficiency of lettuces grown in the partial shade of photovoltaic panels, *Eur. J. Agron.* 44 (2013) 54–66, <https://doi.org/10.1016/j.eja.2012.08.003>.
- [19] H. Marrou, L. Guillion, L. Dufour, C. Dupraz, J. Wery, Microclimate under agrivoltaic systems: is crop growth rate affected in the partial shade of solar panels? *Agric. For. Meteorol.* 177 (2013) 117–132, <https://doi.org/10.1016/j.agrformet.2013.04.012>.
- [20] H. Marrou, L. Dufour, J. Wery, How does a shelter of solar panels influence water flows in a soil-crop system? *Eur. J. Agron.* 50 (2013) 38–51, <https://doi.org/10.1016/j.eja.2013.05.004>.
- [21] M. Homma, T. Doi, Y. Yoshida, A field experiment and the simulation on agrivoltaic-systems regarding to rice in a paddy field, *J. Jpn. Soc. Energy Resour.* 37 (2016) 23–31.
- [22] Y. Elamri, B. Cheviron, J.M. Lopez, C. Dejean, G. Belaud, Water budget and crop modelling for agrivoltaic systems: application to irrigated lettuces, *Agric. Water Manag.* 208 (2018) 440–453, <https://doi.org/10.1016/j.agwat.2018.07.001>.
- [23] R. Mead, R.W. Willey, The concept of a 'land equivalent ratio' and advantages in yields from intercropping, *Exp. Agric.* 16 (1980) 217–228, <https://doi.org/10.1017/S0014479700010978>.
- [24] R.I. Cuppari, C.W. Higgins, G.W. Characklis, Agrivoltaics and weather risk: a diversification strategy for landowners, *Appl. Energy* 291 (2021) 116809, <https://doi.org/10.1016/j.apenergy.2021.116809>.
- [25] Y. Elamri, B. Cheviron, A. Mange, C. Dejean, F. Liron, G. Belaud, Rain concentration and sheltering effect of solar panels on cultivated plots, *Hydrol. Earth Syst. Sci.* 22 (2018), <https://doi.org/10.5194/hess-22-1285-2018>.
- [26] Agromillora, Super High Density - Revolutionary cultivation system that redefine the industry, (n.d.), <https://www.agromillora.com/what-s-the-shd-system/> (accessed July 26, 2021).
- [27] A. Bidram, A. Davoudi, R.S. Balog, Control and circuit techniques to mitigate partial shading effects in photovoltaic arrays, *IEEE J. Photovoltaics* 2 (2012) 532–546, <https://doi.org/10.1109/JPHOTOV.2012.2202879>.
- [28] E. Koutroulis, F. Blaabjerg, A new technique for tracking the global maximum power point of PV arrays operating under partial-shading conditions, *IEEE J. Photovoltaics* 2 (2012) 184–190, <https://doi.org/10.1109/JPHOTOV.2012.2183578>.
- [29] F. Belhachat, C. Larbes, Modeling, analysis and comparison of solar photovoltaic array configurations under partial shading conditions, *Sol. Energy* 120 (2015) 399–418, <https://doi.org/10.1016/j.solener.2015.07.039>.
- [30] J. Antonanzas, R. Urraca, F.J. Martinez-de-Pison, F. Antonanzas, Optimal solar tracking strategy to increase irradiance in the plane of array under cloudy conditions: a study across Europe, *Sol. Energy* 163 (2018) 122–130, <https://doi.org/10.1016/j.solener.2018.01.080>.
- [31] L.M. Fernández-Ahumada, J. Ramírez-Faz, R. López-Luque, M. Varo-Martínez, I.M. Moreno-García, F. Casares de la Torre, A novel backtracking approach for two-axis solar PV tracking plants, *Renew. Energy* 145 (2020) 1214–1221, <https://doi.org/10.1016/j.renene.2019.06.062>.
- [32] L.M. Fernández-Ahumada, J. Ramírez-Faz, R. López-Luque, M. Varo-Martínez, I.M. Moreno-García, F. Casares de la Torre, Influence of the design variables of photovoltaic plants with two-axis solar tracking on the optimization of the tracking and backtracking trajectory, *Sol. Energy* 208 (2020) 89–100, <https://doi.org/10.1016/j.solener.2020.07.063>.
- [33] L.M. Fernández-Ahumada, J. Ramírez-Faz, R. López-Luque, M. Varo-Martínez, I.M. Moreno-García, F. Casares de la Torre, A new methodology to prevent shadows in two-axis solar tracking plants, in: 2019 IEEE Int. Conf. Environ. Electr. Eng. 2019 IEEE Ind. Commer. Power Syst. Eur., EEEIC/I&CPS Eur., IEEE, 2019, pp. 1–4, <https://doi.org/10.1109/IEEEIC.2019.8783819>.
- [34] F.J. Gómez-Uceda, I.M. Moreno-García, J.M. Jiménez-Martínez, R. López-Luque, L.M. Fernández-Ahumada, Analysis of the influence of terrain orientation on the design of pv facilities with single-axis trackers, *Appl. Sci.* 10 (2020) 1–16, <https://doi.org/10.3390/app10238531>.
- [35] N.A. Kelly, T.L. Gibson, Improved photovoltaic energy output for cloudy conditions with a solar tracking system, *Sol. Energy* 83 (2009) 2092–2102, <https://doi.org/10.1016/j.solener.2009.08.009>.
- [36] M. Koussa, A. Cheknane, S. Hadji, M. Haddadi, S. Noureddine, Measured and modelled improvement in solar energy yield from flat plate photovoltaic systems utilizing different tracking systems and under a range of environmental conditions, *Appl. Energy* 88 (2011) 1756–1771, <https://doi.org/10.1016/j.apenergy.2010.12.002>.
- [37] D. Panico, P. Garvison, H. Wenger, D. Shugar, Backtracking, A novel strategy for tracking PV systems, in: Conf. Rec. IEEE Photovolt., Spec. Conf., 1992, <https://doi.org/10.1109/pvsc.1991.169294>.
- [38] G. Quesada, L. Guillon, D.R. Rousse, M. Mehrtash, Y. Dutil, P.-L. Paradis, Tracking strategy for photovoltaic solar systems in high latitudes, *Energy Convers. Manag.* 103 (2015) 147–156, <https://doi.org/10.1016/j.enconman.2015.06.041>.
- [39] J.W. Spencer, Fourier series representation of the position of the sun, *Search 2* (1971).
- [40] F. Martínez-Moreno, J. Muñoz, E. Lorenzo, Experimental model to estimate shading losses on PV arrays, *Sol. Energy Mater. Sol. Cells* 94 (2010) 2298–2303, <https://doi.org/10.1016/j.solmat.2010.07.029>.
- [41] S. Moballegh, J. Jiang, Modeling, prediction, and experimental validations of power peaks of PV arrays under partial shading conditions, *IEEE Trans. Sustain. Energy* 5 (2014) 293–300, <https://doi.org/10.1109/TSTE.2013.2282077>.
- [42] Y.-M. Saint-Drenan, T. Barbier, Data-analysis and modelling of the effect of inter-row shading on the power production of photovoltaic plants, *Sol. Energy* 184 (2019) 127–147, <https://doi.org/10.1016/j.solener.2019.03.086>.
- [43] P.R. Satpathy, R. Sharma, Diffusion charge compensation strategy for power balancing in capacitor-less photovoltaic modules during partial shading, *Appl. Energy* 255 (2019), <https://doi.org/10.1016/j.apenergy.2019.113826>.
- [44] E. Lorenzo, L. Narvarte, J. Muñoz, Tracking and back-tracking, *Prog. Photovoltaics Res. Appl.* 19 (2011) 747–753, <https://doi.org/10.1002/pip.1085>.
- [45] J.A. Duffie, W.A. Beckman, *Solar Engineering of Thermal Processes*, fourth ed., John Wiley and Sons, 2013 <https://doi.org/10.1002/9781118671603>.
- [46] B.Y.H. Liu, R.C. Jordan, A rational procedure for predicting the long-term average performance of flat-plate solar-energy collectors, with design data for the U.S., its outlying possessions and Canada, *Sol. Energy* 7 (1963) 53–74, [https://doi.org/10.1016/0038-092X\(63\)90006-9](https://doi.org/10.1016/0038-092X(63)90006-9).
- [47] J.E. Hay, Calculating solar radiation for inclined surfaces: practical approaches, *Renew. Energy* 3 (1993) 373–380, [https://doi.org/10.1016/0960-1481\(93\)90104-0](https://doi.org/10.1016/0960-1481(93)90104-0).
- [48] R. Perez, P. Ineichen, R. Seals, J. Michalsky, R. Stewart, Modeling daylight availability and irradiance components from direct and global irradiance, *Sol. Energy* (1990), [https://doi.org/10.1016/0038-092X\(90\)90055-H](https://doi.org/10.1016/0038-092X(90)90055-H).
- [49] S.A. Klein, Calculation of monthly average insolation on tilted surfaces, *Sol. Energy* (1977), [https://doi.org/10.1016/0038-092X\(77\)90001-9](https://doi.org/10.1016/0038-092X(77)90001-9).
- [50] R. Posadillo, R. López Luque, A sizing method for stand-alone PV installations with variable demand, *Renew. Energy* 33 (2008) 1049–1055, <https://doi.org/10.1016/j.renene.2007.06.003>.
- [51] M. Gómez-del-Campo, E.R. Trentacoste, D.J. Connor, Long-term effects of row spacing on radiation interception, fruit characteristics and production of hedgerow olive orchard (cv. Arbequina), *Sci. Hortic. (Amst.)* (2020) 272, <https://doi.org/10.1016/j.scienta.2020.109583>.